

Lab on a Chip

Accepted Manuscript



This article can be cited before page numbers have been issued, to do this please use: F. Zheng, Z. Pu, E. He, J. Huang, B. Yu, D. Li and Z. Li, *Lab Chip*, 2018, DOI: 10.1039/C8LC00327K.



This is an Accepted Manuscript, which has been through the Royal Society of Chemistry peer review process and has been accepted for publication.

Accepted Manuscripts are published online shortly after acceptance, before technical editing, formatting and proof reading. Using this free service, authors can make their results available to the community, in citable form, before we publish the edited article. We will replace this Accepted Manuscript with the edited and formatted Advance Article as soon as it is available.

You can find more information about Accepted Manuscripts in the [author guidelines](#).

Please note that technical editing may introduce minor changes to the text and/or graphics, which may alter content. The journal's standard [Terms & Conditions](#) and the ethical guidelines, outlined in our [author and reviewer resource centre](#), still apply. In no event shall the Royal Society of Chemistry be held responsible for any errors or omissions in this Accepted Manuscript or any consequences arising from the use of any information it contains.



Journal Name

ARTICLE

FROM FUNCTIONAL STRUCTURE TO PACKAGING: FULLY-PRINTING FABRICATION OF MICROFLUIDIC CHIP WITHIN BIOSENSORS

Fengyi Zheng,^{a†} Zhihua Pu,^{b†} Enqi He^{a,c}, Jiasheng Huang,^a Bocheng Yu,^a Dachao Li^{*b} and Zhihong Li^{*a}

Received 00th January 20xx,
Accepted 00th January 20xx

DOI: 10.1039/x0xx00000x

www.rsc.org/

This paper presents a concept of FULLY-PRINTING methodology aiming at convenient and fast fabrication of microfluidic devices. For the first time, we achieved a microfluidic biochemical sensor with all functional structures fabricated by inkjet printing, including electrodes, enzyme immobilization, microfluidic components and packaging. With the cost-effective and rapid process, this method provides the possibility for quick model validation of novel lab-on-chip system. In this study, a three-electrode electrochemical system was integrated successfully with glucose oxidase immobilization gel and sealed in an ice channel, forming a disposable microfluidic sensor for glucose detection. This fully-printed chip was characterized and showed good sensitivity and linear section at a low-level concentration of glucose (0-10mM). With the aid of automatic equipment, the fully-printed sensor can be massively produced with low cost.

Introduction

The technology of microfluidics has great impacts on a broad range of areas from biological analysis to chemical synthesis.¹ The microfluidic devices based Lab-on-a-Chip (LOC) possess the advantages of rapid analysis, increased automation, low power consumption, ease of operation, integration capability of multiplexing analysis, and compatibility with mass production.² The LOC enables significant advancement in chemical and biochemical analysis owing to advances in physics, electronics and material science.³ In terms of fabricating or replicating microchannel structures, the dominant techniques utilized in microfluidics can be divided into three main categories: bulk micromachining, surface micromachining and mould machining.⁴ Typically, expensive equipment is necessary for photolithography, deposition and etching in the first two categories, while the third one is strongly dependent on master mould fabrication, which normally needs significantly expensive and time-consuming techniques. However, the high expense and long period fabrication process, on a certain extent, go against the research and development of designing new microfluidic devices. More importantly, for most biological uses,

microfluidic devices are embedded with biofunctional materials such as DNAs, antibodies, enzymes, and hydrogels, which are delicate and prone to be damaged or contaminated by microfabrication processes such as photolithography,⁵ chemical reduction,⁶ evaporation,⁷ sputtering,⁸ lift-off,⁹ bonding,¹⁰ thermal annealing,¹¹ plasma treatment,¹² etc. Therefore, the fixation via double side adhesive tapes¹³ or clamps¹⁴, which is complicated to operate and highly risky in leakage, is required to construct microchannels or reservoirs enclosing biofunctional materials. Alternatively, surface modification and biomolecules immobilization are done after microfluidic structure formation. However, the required biochemical reaction in a long microchannel is time consuming with low efficiency.

In recent years, the up-and-coming inkjet printing technology is arguably the most promising option to address the aforementioned limitations.¹⁵ In this additive manufacturing, only the areas need to be patterned are coated and the process requires no stamp or mask. Besides, the ability to print multiple materials, individually and simultaneously offers great flexibility while designing. Inkjet printing has been proved to be best used in combination with other manufacturing techniques and shows good prospects for development of fully inkjet-printed electrochemical sensors.¹⁶

^a National Key Laboratory of Science and Technology on Micro/Nano Fabrication, Institute of Microelectronics, Peking University, Beijing 100871, China. E-mail: zhhl@pku.edu.cn

^b State Key Laboratory of Precision Measuring Technology and Instruments, Tianjin University, Tianjin 300072, China. E-mail: dchli@tju.edu.cn

^c State Key Laboratory of Tribology, Department of Mechanical Engineering, Tsinghua University, Beijing 100084, China.

† Fengyi Zheng and Zhihua Pu contributed equally to this work.

Electronic Supplementary Information (ESI) available: [details of any supplementary information available should be included here]. See DOI: 10.1039/x0xx00000x

ARTICLE Journal Name

In our previous work, we successfully achieved an additive method for microelectrode patterning using silver nanoparticles on a PDMS substrate¹⁷ and graphene modification on the surface of the working electrode on a polyimide substrate.¹⁸ These two works showed tight bonding between patterns and substrates, and good combination between different layers of patterns. The electrodes also presented good electroactivity and obtained a significantly uniform distribution of electrochemical active sites on the WE electrode surface. On the other hand, a fabrication technology called 3D ICE PRINTING was proposed to provide a bio-friendly method for chemical biosensor fabrication.¹⁹ The process environment of 3D ICE PRINTING with low temperature and nitrogen atmosphere was beneficial to enzyme immobilization in hydrogel.²⁰ Based on inkjet-printed electrodes technology and 3D ice-printing technology, we pioneer a fully printing fabrication method, aiming at fabricating the whole structure of lab-on-a-chip and microfluidic device by inkjet printing with aqueous solution of different materials as ink. This method endows ice sacrificial layers not only the indicating solution but also the protective layer of biological sample pre-sealed in the chip. Graphics of different materials and structures are designed in the same coordinate system layer-by-layer using CAD software to reach alignment. Consequently, more sophisticated 3D ice structures with fine feature sizes and even enzyme embedded gel patterns can be integrated by processing the layer-by-layer printing sequences. On the basis of our proposed fully printing method, we successfully fabricate the glucose detection microfluidics chip as a significant supplement to our previous work.^{18, 21} This fully printed chip shows good sensitivity and linear section at a low-level concentration of glucose (0-10mM). With the aid of automatic equipment, this kind of chip can be massively and cost-effectively produced and enables the evolution of highly efficient and versatile analytical tools in the biomedical field.

Principle

In this paper, we take a glucose detection sensor as a demo of fully-printing fabrication method. Figure 1(a) demonstrates the schematic view of the designed sensor, which consists of a testing area, a straight ice channel acting as microfluidics for sample injecting and a photopolymer as an encapsulation layer. The testing area and the microfluidics are entirely fabricated by inkjet printing. As shown in Figure 1(b), the structure of the testing area has three layers, including a three-electrodes system, a piece of immobilized glucose oxidase gel, an ice structure channel connected with the microfluidics. Both the working electrode and the reference electrode are $200\ \mu\text{m} \times 1000\ \mu\text{m}$, and the counter electrode is $1000\ \mu\text{m} \times 1000\ \mu\text{m}$. All the three leads are $100\ \mu\text{m} \times 5000\ \mu\text{m}$ and the pads are $1000\ \mu\text{m} \times 1000\ \mu\text{m}$. The gel with immobilized enzyme acts as electrochemically sensing material and covers the WE electrode. A $500\ \mu\text{m}$ width ice line, printed by ice printing technique, runs through the gel and forms a $300\ \mu\text{m}$ height microfluidic channel after the solidification of 2 mm thick sealing photopolymer. The low-temperature environment

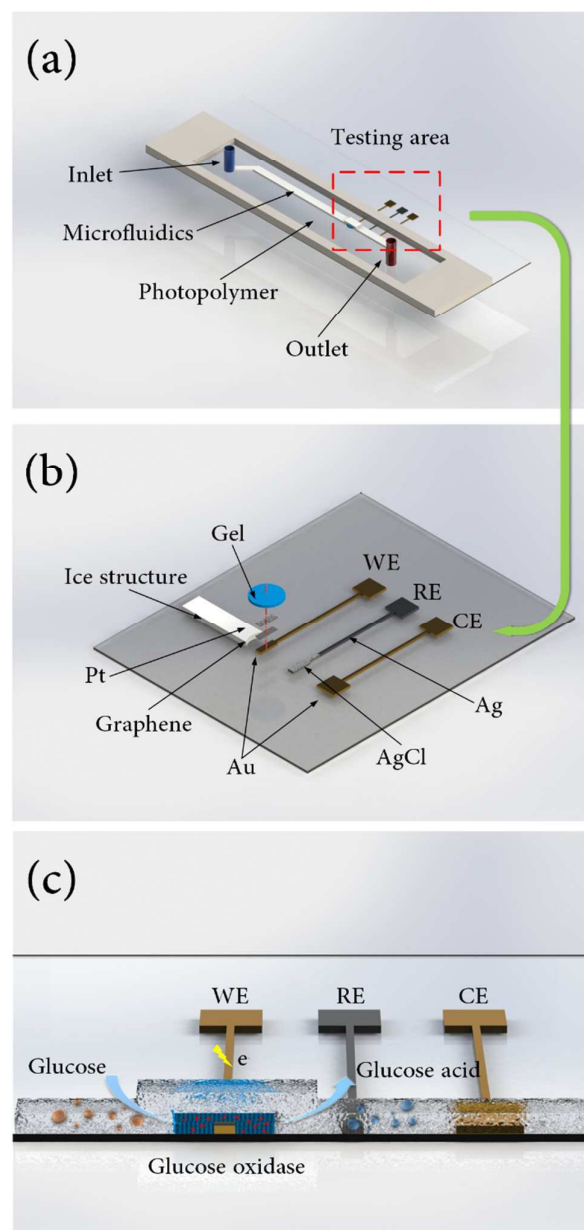


Figure 1: The schematic view of a fully-printing glucose sensor. (a) The complete sensor; (b) Detail of the printed structure. (c) Schematic diagram of the electrochemical sensor for glucose measurement and its integration into a fully-printing chip.

during the fabrication process and the preservation protects the biological activity of the glucose oxidase. When it comes into testing in room temperature, the ice structure melts and forms a channel with buffer in it. The glucose solution fully fills the microfluidic channel and diffuses into the porous structure of the hydrogel to conduct the catalytic reaction. The electric current of reaction can be detected by the ammeter connected with the leads of the electrodes.

Method

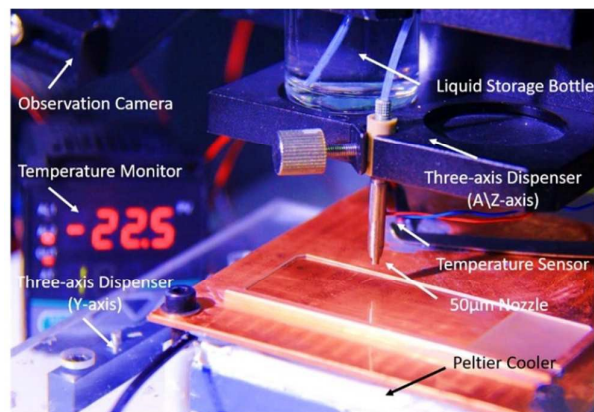


Figure 2: The self-built ice-printing system.

Printing system.

Two self-built printing systems, an ice-printing system as shown in Figure 2 and a nanomaterial printing system similar to that shown in the previous work¹⁸, are used together to enable the fabrication of the proposed fully-printing microfluidic chip. Both of the two self-built printing systems consist of four parts: the printing module, the three-axis mobile robot, the temperature control system and the observation module. The printing module, made up of piezoelectric printheads (one with the nozzle diameter of 50 µm for the ice-printing system, four with the nozzle diameter of 30µm for the nanomaterial printing system), an electric controller and a waveform control software, is purchased from MicroFab Technologies, Inc., USA.

The three-axis mobile robot is custom-made from Ruidu Photoelectric, Inc., Shanghai, which provides the convert software for CAD graphic to execution program, the three-dimension movement, and the localization of the position relationship between the nozzle and the substrate. The temperature control system consists of two subsystems, a hot plate for heating and a Peltier cooler for freezing (the nanomaterial printing system contains a hot plate only while the ice-printing system contains both of them). The two subsystems are both covered with a latten to ensure the evenness of temperature on the surface of the substrate. The temperature is monitored by a Pt-1000 thermistor connected with a digital temperature meter. The observation module includes a diagonally positioned camera and a strobe, which allows us to observe the printing status as well as calibrate the start-point for printing.

Similar to the previous ice-printing work we have done in 2015, we put the whole ice-printing system in a windtight glove box to control the humidity and the oxygen content by adjusting the influx and outflow rate of nitrogen. Low humidity contributes to the shape maintenance of ice printing pattern. Isolation of oxygen is necessary for copolymerization of most gels.

The pattern control of nanoparticles printing.

Different nanomaterials require different parameters of printing, including the voltage of the piezoelectric nozzle, the

space between each printed droplet and the temperature of the substrate. Firstly, ink of nanomaterial with high viscosity needs a higher peak-to-peak value of voltage to generate regular droplets without satellites. Secondly, ink with high viscosity also needs a bigger space between the droplets on the substrate. Because the diameter of the droplet will get bigger when it crashes onto the substrate²² and the viscous liquid changes more significantly. In order to form a smooth edge, the droplets should always fall on the circumference of the prior imprinting marks. The empirical estimates of the size of the droplets for Au nanoparticles and Ag nanoparticles on glass slides are 95 µm and 65 µm. Thirdly, ink with high viscosity needs a relative low substrate temperature to reach a lower rate of evaporation as it takes longer time for the droplets coming into film driven by surface tension²³. Our experiments show that the suitable time and temperature for Au are 30 minutes with 200-degree C and for Ag are 10 minutes with 220-degree C.

Generally, the film formed by nanoparticles of Au/Ag/Graphene needs a postbaking in a higher temperature to make the nanoparticles get a secondary fusion, which will markedly enhance the compactness of the film and the adhesion to the substrate. The temperature and time of postbaking depend on the material of nanoparticles.

The challenge of ice-printing in microfluidic fabrication.

Here we improve the ice printing ability of our previous work to make the ice structure can be customized and used for graphical representations of functional microfluidics. The major challenge in the development of fully printing method is controlling three-dimension structures of ice, which is mainly influenced by the space between every two droplets l . As the printing frequency f and the velocity of the nozzle v are the only two parameters we are able to control in the software, the key is to find the specific relationship between l , v and f . When a line segment of L in length is made up of n droplets, it is obviously that l equals L divided by n . The number of droplets n equals f multiplied by the printing time t , while t equals the distance L divided by the velocity of the nozzle v . According to the above-mentioned relationship, we get the following equation between l and the ratio of velocity to frequency:

$$l = \frac{L}{n} = \frac{L}{f \cdot t} = \frac{L}{f \cdot L/v} = \frac{v}{f}$$

Affected by surface tension, the droplets on the surface of the substrate will gather into a bigger droplet when l is smaller than its diameter d . The bigger the droplet is, the slower it is frozen into ice, then the bigger liquid phase droplet will adsorb other small droplets. Meanwhile, when l is too big, the line segment will be discontinuous instead of the designed shape. Experimental results demonstrate that the proper l_0 is between 0.7 d and 1.2 d , considering the height reduction of the edge of the ice pellets and the volume expansion during the frozen process.

Another challenge is the supercooling water phenomenon. Supercooling is the process of lowering the temperature of a

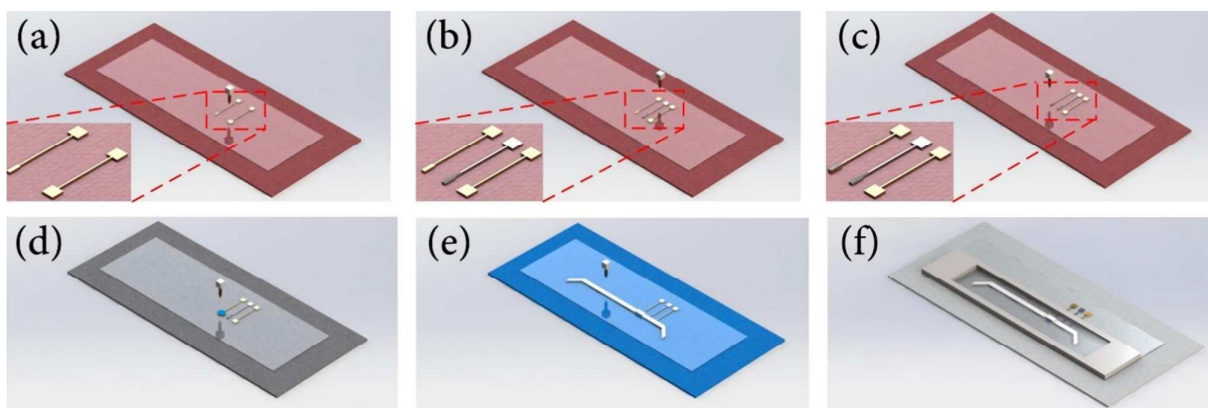


Figure 3: Fabrication process of fully-printing glucose sensor. (a) Printing of the Au patterns, including the first layer of work electrode (left) and the counter electrode (right); (b) Printing of the Ag patterns, which acts as the reference electrode. FeCl_3 was dropped on one side of the electrode for 20 seconds to form AgCl ; (c) Printing of GOx and Pt to finish the modification of the work electrode; (d) Printing of the glucose oxidase embedded gel; (e) Printing of the ice channel; (f) Packaging by photopolymer.

liquid or a gas below its freezing point without solidification. In our work, we find that micro droplets crashing onto the cold surface are easy to freeze while large droplets are more likely getting into an amorphous (non-crystalline) solid. Meanwhile, a liquid crossing its standard freezing point will crystallize in the presence of a seed crystal or nucleus around which a crystal structure can be formed through solidification. Thus the ice patterns must be printed in two steps. We first set the printing process at low frequency to make the microscale droplets arranged in lines quickly freeze into an ice trace. The ice trace acts as ice nucleus in the second printing process to avoid supercooling phenomenon. As the second printing process is in a high printing frequency, it fast fills up the ice structure in the z-axis.

Experimental

Chemicals.

Gold nanoparticles ink was bought from UT Dots, Inc., USA. Silver nanoparticles ink and reduced graphene oxide (RGO) ink were purchased from Sigma Aldrich. Platinum nanoparticles ink was obtained from Changchun Institute of Applied Chemistry Chinese Academy of Sciences. Glucose oxidase (GOx , Type X-S, lyophilized powder, 100 units/mg), acrylamide and N,N-methylene bis-acrylamide were obtained from Sigma-Aldrich (ST. Louis, MO). Riboflavin, Potassium, sodium chloride (NaCl), Sodium phosphate dibasic dodecahydrate ($\text{Na}_2\text{HPO}_4 \cdot 12\text{H}_2\text{O}$), monobasic potassium phosphate (KH_2PO_4) and potassium chloride (KCl) were purchased from Beijing Chemicals (Beijing, China).

Other equipment and materials we used are as follows: Peltier cooler, digital thermometer and hygrometer, light cure medical adhesive (Loctite 3311), clear float glass slides, poly (methyl methacrylate) (PMMA).

Function	Component	Concentration	Dosage
Stock solution of monomer	Acrylamide	400 mg/mL	1 mL
Crosslinking reagent	N,N-methylene bis-acrylamide	23 mg/mL	4 mL
Enzyme solution	Glucose Oxidase	5 mg/mL	1 mL
Photo-catalyst	Riboflavin	0.3 mg/mL	100 μL
Crosslinking catalyst	Potassium persulfate	0.3 mg/mL	100 μL

Table 1: The recipe of the gel embedding the enzyme

Figure 3 demonstrates the schematic view of the fabrication process of fully printing method, which could be divided into four steps according to the temperature variation of the substrate. The optical photograph of the completed chip is illustrated in Figure 4(a).

Printing and modification of the electrodes.

First of all, the slide of float glass was cleaned with ethyl alcohol and dealt with Corona. Then the substrate was heated to 120-degree C by a hot plate and the three electrodes of the electrochemical biosensor were inkjet printed on it. The printing process consisted of three steps, as shown from Figure 3(a) to Figure 3(c). Firstly, the nano-gold ink was printed to form the working electrode and the counter electrode. These two electrodes required a postbaking for fifteen minutes at 210-degree C. Secondly, the nano-silver ink was patterned as the reference electrode and was postbaked for ten minutes at 210-degree C. Next, the ferric chloride was dropped on the pad of the reference electrode for twenty seconds to complete the chlorination and then was washed away by ultrapure water. Thirdly, the RGO ink was sprayed on the pad of working electrode to improve the detection of weak glucose signals, and the Pt nanoparticle solution was printed on the layer of RGO to enhance the electron-mobility of the electrode.¹⁸ The layer of Au and Pt was printed twice to ensure that the film of the electrode had no flaw of holes and the layer of graphene was just printed once.

Printing and immobilization of enzymes on the work electrode.

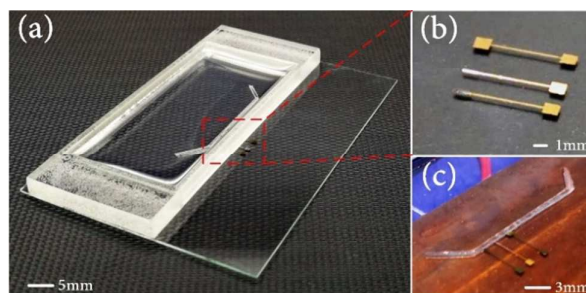


Figure 4: (a) The completed glucose detection chip. (b) The detail of the printed electrodes. (c) The detail of the ice structure running through the electrodes.

try 20xx

adjust margins

Journal Name ARTICLE

Table 1 shows the recipe of the required solution. 0.1 M standard phosphate buffer (PBS, pH = 7.4) was prepared by dissolving 8 grams of NaCl, 2.89 grams of Na₂HPO₄·12H₂O, 0.2 grams of KH₂PO₄ and 0.2 grams of KCl in 1 L of ultrapure water. All the solutions were diluted with PBS and were used right after they were ready. The gel was prepared by mixing 1 mL of the stock solution of monomer with 4 mL of the crosslinking reagent. The reagent mixture was deoxygenated in a vacuum air-removed pot before the addition of the glucose enzyme to

avoid the oxygen inhibition of the copolymerization. Then 1 mL of enzyme solution, 100 µL of photo-catalyst and 100 µL of crosslinking catalyst were added into the gel solution respectively. Because small volume of potassium persulfate was not able to catalyse the polymerization while a further quantity of initiator would harm the enzyme activity, the photoinitiator was combined with potassium persulfate to make a balance between the speed of catalysis and the preservation of biological activity.

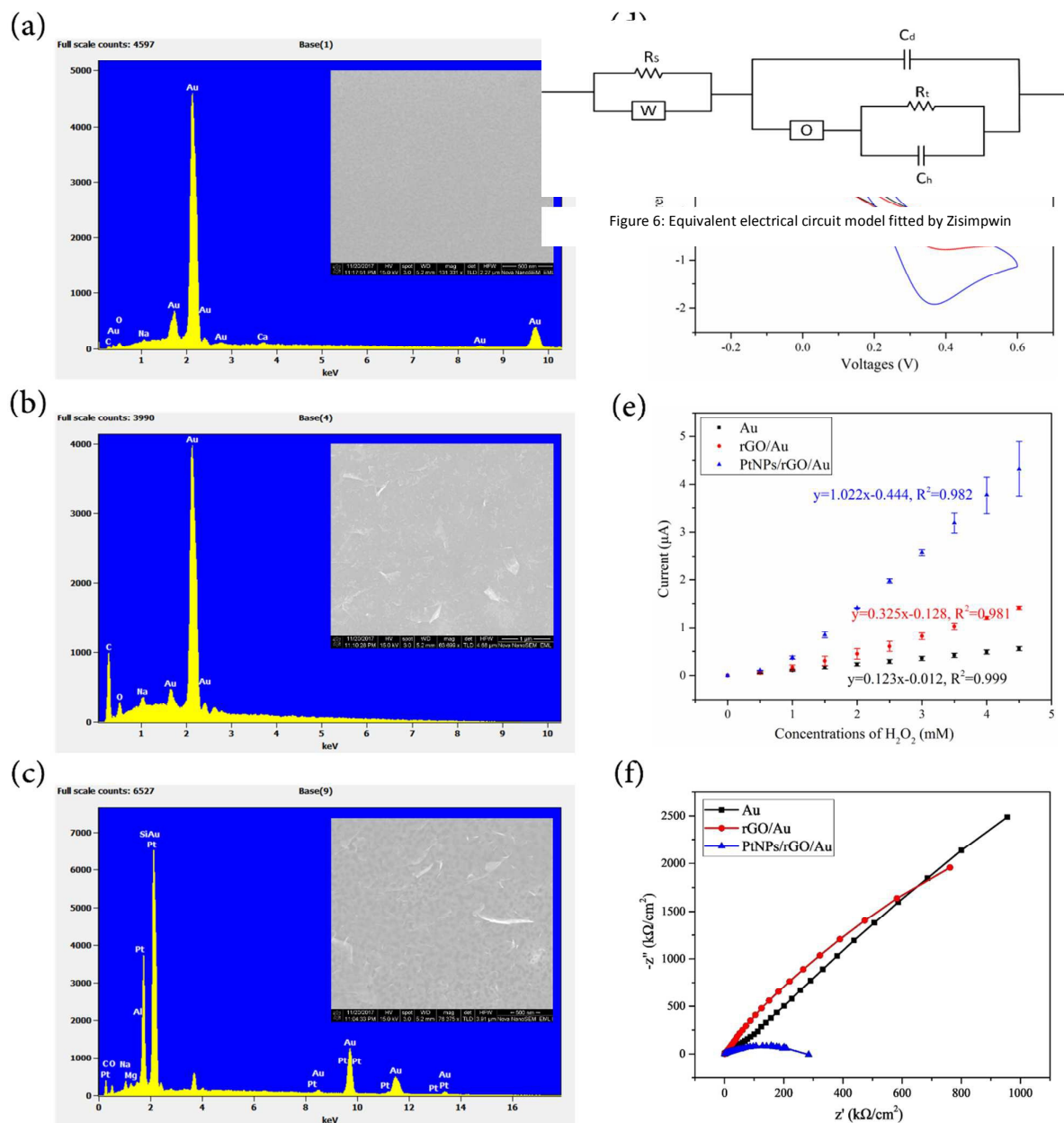


Figure 5: Characterization of the electrodes. The optical photographs and SEM images of (a)Au; (b)Graphene; (c)Pt; (d) the cyclic voltammety characteristics of the three-electrode sensor; (e) the typical amperometric responses of the various sensor configurations to successive increment of 0.5mM H_2O_2 at an applied potential of -0.2 V; (f) the Nyquist diagram of the EIS test for different configurations of WE.

The pattern of the gel solution was designed in a circular shape with a diameter of 500 μm , which totally covered the pad of the work electrode. As the operation box was full of nitrogen, the anaerobic copolymerization proceeded rapidly when a 365 nm LED (7 watts) exposed on it and was completed in twenty minutes, with the end point defined as the time taken for the gel to reach maximum opacity. The wave length of 365nm belonged to ultraviolet a (UVA). On the one hand, the penetrability of UVA was weak and its half-life period was much shorter in the water diluted solution than in the air. So it

will only do little damage to the enzyme. On the other hand, the activity of enzyme depended on its active site. Enzyme immobilization in gel benefited the stability of enzyme structure. Compared with structural damage in membrane structure with enzyme on the electrodes, the cost by UVA exposure was worthy. (ESI Figure S1) Meanwhile, the temperature of the Peltier cooler was set to 0-degree C to reduce the effect of heat denaturation of the enzyme during the exothermic reaction.

Printing and patterning of the ice channel.

Next, the temperature of the Peltier cooler was adjusted to minus 25-degree C. Ultrapure water was printed on the substrate and was frozen into the ice channel. The width of the ice channel, which ran through the circular disk of the gel, was designed to be 300 μm to avoid the movement of the gel in the microfluidic channel. As a single ice line formed by printing was about 150 μm , the ice channel was designed in two parallel segments with a gap of 150 μm .

The printing process was divided into two steps. First, we set the velocity of the nozzle to 6 mm/s and frequency of the injection to 60 Hz with a circulation of five times in order to form the basic outline of the pattern. Then we printed the same pattern with a velocity of 20 mm/s and frequency of 500 Hz with a circulation of ten times to make the structure of ice in a higher-order structure. The height of the ice channel can reach 300 μm after the entire printing process.

Packaging of the sensor.

Finally, a square cofferdam, which surrounded the area of sensor, was placed on the substrate, and the photopolymer precursor was added and polymerized to seal the electrode, gel as well as the ice channel. Compared with PDMS, Light-sensitive adhesive had fast curing speed and better adhesiveness to the substrate. Following consideration of the biocompatibility, transparency and Young modulus, here we selected Loctite 3311, a medical grade light-sensitive adhesive, as packaging materials. Furthermore, Loctite 3311 had a low followability in low temperature environment and will not drain out of the cofferdam. Upon exposure to a 420 nm LED lamp (7 watts), the curing process was completed in three minutes at minus 25-degree C.

Preservation and testing.

The chip could be preserved in minus 4-degree C to keep the biological activity of the glucose oxidase in the gel. Holes were punched at the beginning and the ending of microfluidic channel as inlet and outlet when the chip was used at room temperature (22-degree C). Reaction agent was injected into the chip through a flexible tube by a peristaltic pump. As the glucose oxidase was immobilized in the gel, the flowing solution did not contact the enzyme directly. The catalytic reaction began when the glucose solution diffused into the porous structure of the gel. In this case velocity is not the main influence in the diffusion process when the microfluidic channel is full filled. The bared pads of electrodes were connected to a galvanometer by copper wire fixed on them with conducting resin. The chip was disposable as the fabricate method was cost-effective and can be massively produced easily.

Results and discussion

Characterization of electrodes.

Physical characterization is illustrated in from Figure 5(a) to Figure 5(c). Optical photographs and SEM images show that printing method enables to make continuous uniform film. The energy spectrum (EDS) demonstrates that medium arranges

layer by layer as designed and has good stability and binding ability.

As shown in Figure 5(d), the cyclic voltammetry characteristics of the three-electrode sensor satisfy the requirement of electrochemical detection in microfluidics chip. Each layer of material printed on the WE surface was first tested using the amperometric technique. H_2O_2 was utilized to characterize the electrodes because it was generated as the decomposition of glucose by immobilized glucose oxidase (GOx). Figure 5(e) shows the typical amperometric responses of the various sensor configurations to successive increment of 0.5 mM H_2O_2 at an applied potential of -0.2 V. As shown in Figure 5(e), the electrochemical response increases as the H_2O_2 concentration increases, and all of the sensors demonstrate good linearity from 0 to 4.5 mM H_2O_2 . Furthermore, the Nyquist diagram of the EIS test for different configurations of WE is shown in Figure 5(f), where 5mM potassium ferricyanide ($\text{K}_3[\text{Fe}(\text{CN})_6]$) in 0.1 M PBS was employed as determinand, 500 mV DC and 10 mV AC potentials vs Ag/AgCl were applied between WE and CE with frequencies from 0.1 Hz to 100 kHz. Figure 6 shows the equivalent electrical circuit model fitted by Zisimpwin. R_s , W , O , R_t , Ch and Cd represents the impedance of the solution between WE and RE, the semi-infinite diffusion impedance of WE, the finite layer diffusion impedance of WE, the electron transfer resistance of WE, the capacitance of the Helmholtz capacitor of WE and the capacitance of the double-layer capacitor of WE, respectively. The electron transfer rate significantly affected the sensitivity. According to the measured electrochemical impedance spectroscopy and the obtained equivalent electrical circuit model, the R_t values of the three kinds of WE were calculated as 44.55k Ω/cm^2 (Au), 13.85k Ω/cm^2 (rGO/Au) and 0.13k Ω/cm^2 (PtNPs/rGO/Au). The WE with rGO and Pt nanoparticles held the smallest electrochemical impedance so that enhanced the electrons transfer rate of the WE to satisfy low levels of glucose measurements.

Evaluation of the fully-printing glucose sensor.

In this paper, the sensitivity and the linearity of the glucose

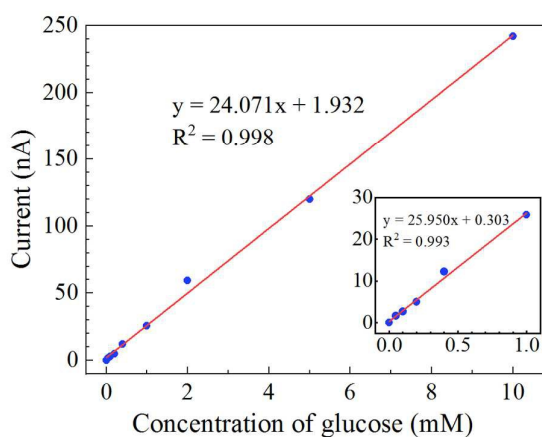


Figure 7: Result of the measurement with the fully-printing glucose sensor (room temperature, 22-degree C).

ARTICLE Journal Name

measurements were evaluated to prove that fabrication of fully-printing biosensor was feasible. The interlayer of graphene improved the detection of weak glucose signals. Pt nanoparticles modified onto the WE surface improved the electroactive nature and obtained a more uniform distribution of electrochemically active sites on the electrodes to enable measurements of glucose.¹⁸ The detection limit were measured by successively increasing 0.01 mM glucose at an applied potential of 0.4 V and the first efficient signal was found at 0.05 mM. Then the experiments were conducted by detecting several representative points. Figure 7 demonstrates that the current signals of the reaction with different levels of glucose, which agrees with linear relation from 0 mM to 10 mM.

Future utility of the presented chip manufacturing method.

For research in private laboratories, the proposed printing system can be reproduced as a desktop equipment for manufacture of microfluidics chip. By leveraging the flexibility and compatibility of inkjet printing, different structures can be achieved by designing graphics in CAD software. Thus, technicians can easily get a chip demo with ice structure taking place of the reverse mould, and electrodes taking place of electroplating and magnetic sputtering. The method, which gets rid of complicated fabrication processes in ultra-clean room, such as photolithography, remarkably reduces the fabrication cost.

In addition, fully-printing method has great potential in industrial manufacture. Each printing step is independent and can be projected in an assembly line. Taking the glucose sensor in this paper as example, although it takes nearly an hour to fabricate one chip, at most ten chips could be produced in an hour with four printing systems. The production per hour is only limited by the longest printing step in the whole process.

Conclusions

In this paper, we proposed a cost-effective and timesaving fully-printing method based on layer-by-layer inkjet printing, which was appropriate for mass production of chemical biosensors. This method showed good integration capabilities of different materials and structures with different geometry, sizes, height and layers. By utilizing a commercially available printer and commonly used CAD software, the inkjet printing system significantly reduced the expense of both equipment and technological process, and was easy to be reproduced at private laboratories.

Furthermore, multi-function analysis can be realized by constructing different gel environment in different places and different layers for different targets on one microfluidic chip. Particularly, a more complex structure with more layers in different patterning can be designed to process functions such as extraction, transmission, volume measurement and storage into a highly integrated microfluidic chip.

A glucose detection chip sensor for microfluidic sensing was fabricated successfully using inkjet printing from functional

structure to packaging. So was integrated lab-on-a-chip system. The system implemented the three-electrode electrochemical sensor, enzyme embedded gel as biochemical reactor all in one microfluidic chip. The work here described a new direction for fabricating functionalized microfluidics chips. The fully-printing fabrication method might offer the potential to be applied in industrial manufacturing, as the operating mode could be designed into a full-automatic flow line production.

Author contributions

F.Y. Zheng, Z.H. Pu and E.Q. He conceived the idea of the study; F.Y. Zheng, Z.H. Pu and J.S. Huang performed the research; Z.H. Pu and B.C Yu collected and analysed data; F.Y. Zheng wrote the initial draft of the paper; all authors discussed the results and revised the manuscript.

Conflicts of interest

There are no conflicts to declare.

Supplementary Material

Refer to Web version on PubMed Central for supplementary material.

Acknowledgements

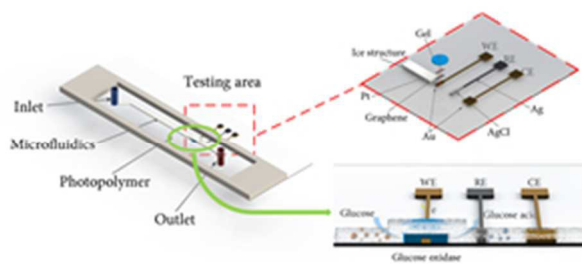
This work was supported by the National Key Research and Development Program of China (No. 2016YFA0200802 and No. 2017YFA0205103) and the National Natural Science Foundation of China (No. 91323304 and No.81571766).

References

- Whitesides, G.M., *Nature*, 2006. **442**(7101): 368-373.
- Zhang, Y., S. Ge, and J. Yu, *Trac Trends in Analytical Chemistry*, 2016. **85**: 166-180.
- Wu, J., Q. Chen, W. Liu, Z. He, and J.M. Lin, *Trac Trends in Analytical Chemistry*, 2016. **87**.
- Glavan, A.C., D.C. Christodouleas, B. Mosadegh, H.D. Yu, B.S. Smith, J. Lessing, and G.M. Whitesides, *Analytical Chemistry*, 2014. **86**(24): 11999-2007.
- Pearce, J.M., *Science*, 2012. **337**(6100): 1303-1304.
- Zhang, Q., J.J. Xu, Y. Liu, and H.Y. Chen, *Lab on A Chip*, 2008. **8**(2): 352-357.
- Pandya, H.J., S. Chandra, and A.L. Vyas, *Sensors & Actuators B Chemical*, 2012. **161**(1): 923-928.
- Feng, J.T. and Y.P. Zhao, *Biomedical Microdevices*, 2008. **10**(1): 65.
- Z, N., N. CA, G. J, C. X, K. A, M. AW, N. M, and W. GM, *Lab on A Chip*, 2010. **10**(4): 477-483.
- Bhattacharya, S., A. Datta, J.M. Berg, and S. Gangopadhyay, *Journal of Microelectromechanical Systems*, 2005. **14**(3): 590-597.

Journal Name ARTICLE

- 11 Sheng, Z.H., L. Shao, J.J. Chen, W.J. Bao, F.B. Wang, and X.H. Xia, *Acs Nano*, 2011. **5**(6): 4350-4358.
- 12 Li, X., J. Tian, T. Nguyen, and W. Shen, *Analytical Chemistry*, 2008. **80**(23): 9131-4.
- 13 Blake, A.J., T.M. Pearce, N.S. Rao, S.M. Johnson, and J.C. Williams, *Lab on A Chip*, 2007. **7**(7): 842-849.
- 14 Pu, Z., C. Zou, R. Wang, X. Lai, H. Yu, K. Xu, and D. Li, *Biomicrofluidics*, 2016. **10**(1): 011910.
- 15 Wang, H., J. Liu, X. Zheng, X. Rong, X. Zheng, H. Peng, Z. Silber-Li, M. Li, and L. Liu, *Scientific Reports*, 2015. **5**: 10945.
- 16 Moya, A., G. Gabriel, R. Villa, and F.J.D. Campo, *Current Opinion in Electrochemistry*, 2017.
- 17 Wu, J., R. Wang, H. Yu, G. Li, K. Xu, N.C. Tien, R.C. Roberts, and D. Li, *Lab on A Chip*, 2015. **15**(3): 690.
- 18 Pu, Z., R. Wang, J. Wu, H. Yu, K. Xu, and D. Li, *Sensors & Actuators B Chemical*, 2016. **230**: 801-809.
- 19 Zhang, H., H. Li, M. Wu, H. Yu, W. Wang, and Z. Li. in *IEEE International Conference on MICRO Electro Mechanical Systems*. 2014.
- 20 Hicks, G.P. and S.J. Updike, *Analytical Chemistry*, 1966. **38**(6): 726.
- 21 Fengyi Zheng, Z.P., Enqi He, Dachao Li and Zhihong Li, in *The 21st International Conference on Miniaturized Systems for Chemistry and Life Sciences (MicroTAS 2017)*. 2017: Savannah, USA. p. 761.
- 22 Asai, A., M. Shioya, S. Hirasawa, and T. Okazaki, *Journal of Imaging Science & Technology*, 1993. **37**(Suppl 6): 205-207.
- 23 Khan, M.S., D. Fon, X. Li, J. Tian, J. Forsythe, G. Garnier, and W. Shen, *Colloids & Surfaces B Biointerfaces*, 2010. **75**(2): 441-447.



79x39mm (96 x 96 DPI)